IAC–17–B4,3,12,x41638

# SmallSat Navigation via the Deep Space Network: Lunar Transport

**Jeffrey Stuart**
Jet Propulsion Laboratory, California Institute of Technology, USA, jeffrey.r.stuart@jpl.nasa.gov

**Lincoln Wood**
Jet Propulsion Laboratory, California Institute of Technology, USA, lincoln.j.wood@jpl.nasa.gov

Spacecraft component miniaturization, the standardized CubeSat form factor, and a corresponding increase in launch ride-share availability have led to a renewed interest in smaller, more agile spacecraft missions. Naturally, interest in SmallSat capabilities extends outside of low Earth orbit for a variety of science and technology demonstration applications. As with larger missions, near-term deep-space SmallSats will more than likely rely on telecommunications and tracking via NASA's Deep Space Network or similar facilities. Given the predicted growth in the number of deep space missions, effective use of telecommunication resources will be more critical than ever, even with Multiple Spacecraft Per Aperture capability. In particular, SmallSat missions will likely face stricter limitations on two-way contact with the tracking stations, thus making other options like one-way data types more attractive. While all missions must eventually develop their own detailed navigation plans, a common set of references is needed to support SmallSat missions, especially in the early development phases. Our investigation provides this initial survey of expected navigation performance for standard radiometric data types, from traditional two-way Doppler and ranging capabilities to one-way equivalents, including delta-differential one-way range. In this investigation, we examine transport within the Earth-Moon region, the first step outward from Earth into deep space exploration.

## I. Introduction

The cost of launch into orbit presents one of the greatest barriers to access to space, with large launch vehicles required for even relatively modest payload masses. On the other hand, the miniaturization of spacecraft components, and the CubeSat form factor in particular,[1] has lead to a renewed interest in smaller, more agile missions within the space community. Couple this interest with the proliferation of rideshare opportunities easing access to orbit for smaller payloads and it's no wonder that we have seen an explosion in the number of operational SmallSats in Earth orbit. Naturally, the interest in SmallSat capabilities extends outside of LEO, with JPL alone planning to fly MarCO,[2] INSPIRE,[3] Lunar Flashlight,[4] and NEAScout[5] beyond Earth orbit. As with larger missions, deep-space SmallSats will more than likely rely on the telecommunications and tracking capability of the Deep Space Network (DSN) or similar entities. Given the predicted growth in the number of deep space missions, we expect that DSN resources will be in high demand, even with the upcoming capability to support Multiple Spacecraft Per Aperture (MSPA).

As a general rule, SmallSat missions are cost effective because rideshare opportunities are cheaper than dedicated launches and a common form factor encourages the development and compatibility of off-the-shelf components. A common misconception, however, is that these cost savings necessarily extend to all aspects of the mission, including operations and telecommunications. For example, costs for mission design and navigation are directly tied to the complexity of the mission as well as the attendant navigation requirements and are nearly insensitive to the actual size of the spacecraft. In fact, it is entirely conceivable that a SmallSat mission could levy more stringent position or velocity knowledge requirements than a mission with a larger spacecraft. Accordingly, any savings in operational cost, effort, or DSN use will more than likely arise from careful assessment of the mission class, the relevant risk posture, and any associated impacts on or relaxation of operational requirements. While all missions will eventually develop their own detailed navigation plans, a common set of references is needed to support SmallSat missions, especially in the early development phases.

While there is an extensive literature on the subject of deep-space navigation, most works focus on analyzing specific mission concepts and are not broad surveys of navigation capability. Lincoln Wood has authored a series of papers detailing the historical development of deep space navigation, covering trends

and specific missions up to 2006.[6–9] Even these literature surveys, however, don't present DSN tracking options in a convenient format for perusal and selection by future missions. Our current investigation seeks to address this need for a high-level view of the navigation performance that SmallSat missions can expect when using the DSN. We cover a broad range of tracking scenarios utilizing multiple different measurement types:

1. two-way Doppler and ranging measurements;
2. the equivalent one-way measurements enabled by precise on-board clocks; and
3. Delta Differential One-way Ranging (DDOR).

The performance of one-way tracking is of particular interest because this measurement type can exploit MSPA; multiple spacecraft can downlink to the ground station while one satellite is receiving uplink. Our goal is to provide a catalogue of options for DSN support, with reasonable performance estimates, which prospective SmallSat missions can use to predict required staffing and funding levels for their own development and operational needs. The following sections detail our analysis approach as well as qualitative discussions of the results for various tracking scenarios; the appendix contains comprehensive tabulations of the results.

## II. Navigation Simulation Approach

To characterize navigation performance, we investigate state reconstruction and prediction accuracy using straight-forward covariance analysis; a detailed mathematical description of this analysis technique can be found in Chapter 6 of *Statistical Orbit Determination*.[10] We focus on characterizing the performance associated with traditional measurements from the DSN ground stations at Goldstone, Madrid, and Canberra, although our results should be broadly applicable to similar international and domestic partner sites. We performed all trajectory and navigation simulations using JPL's Mission Analysis, Operations, and Navigation Toolkit Environment (MONTE);[11] planetary ephemerides are provided by JPL's HORIZONS database.[12]

### II.i Traditional Two-Way Radiometric Data Types

Two-way Doppler range-rate is perhaps the most commonly used data type supplied by the DSN. Two-way Doppler measurements originate as a signal transmitted by one of the DSN ground stations; spacecraft receive this signal then relay it back to the transmitting antenna on Earth. Measured differences in frequency between the transmitted and the received signals are subsequently translated to spacecraft line-of-sight velocity estimates. Given sufficiently long tracking passes, two-way Doppler measurements provide a wealth of information about the spacecraft orbital motion as well as the surrounding dynamical regime.[13] Indeed, such tracking information is the primary data type for host of planetary gravity science investigations. Similarly, two-way ranging is available through the DSN via the Sequential Ranging Assembly (SRA), which converts two-way light times into range units. Throughout this investigation we will use the acronym SRA to refer primarily to the two-way ranging data provided by the ranging assembly, though technically SRA refers to the hardware system. However, two-way measurements necessarily require dedicated support from a DSN antenna for the duration of a tracking pass, limiting their availability as the number of spacecraft in operation grows larger. Furthermore, SmallSat missions might be considered of lower priority than larger missions, meaning that already sparse tracking schedules may be disrupted if a higher priority mission needs to recover from a safe mode or other upset event. Thus, we also consider the use of alternate data sources, specifically one-way Doppler, one-way Range and Differential One-Way Range (DDOR). Brief descriptions of these data types are presented in the following sections; more rigorous mathematical treatments of the data types can be found in Moyer,[14] with DSN specific data provided by the DSN Link Design Handbook.[15] For this investigation, uplink and downlink are both assumed to be X-band, regardless of the specific measurement type used; the data weights used for our analysis are presented in Table 1.

Table 1: Data weights used for covariance simulation, all noises 1-$\sigma$.

| **Parameter** | **Value** | **Units** |
|---|---|---|
| X-band frequency | $7.9\times10^{9}$ | Hz |
| Two-way Doppler noise | $5.62\times10^{-3}$ | Hz |
| Two-way SRA noise | 1.0 | m |
| One-way Doppler noise | $8.17\times10^{-2}$ | Hz |
| One-way range noise | 5.0 | m |
| CSAC white noise (1-day) | $2.15\times10^{-3}$ | Hz |
| CSAC random walk (1-day) | $6.44\times10^{-2}$ | Hz |
| CSAC Allan deviation (1-day) | $4\times10^{-11}$ | s/s |
| DDOR noise | 0.06 | ns |

### II.ii Modeling of One-Way Radiometric Tracking

Opportunistic use of one-way Doppler tracking via the DSN's Multiple Spacecraft Per Aperture (MSPA) capability may provide an alternative data source for state estimation, one that can take advantage of a tracking pass whose primary target is another spacecraft. In contrast to two-way measurements, we model one-way measurements as originating on the spacecraft and being received by ground stations; for antennas that can receive and record multiple signals, tracking data for multiple spacecraft can be simultaneously captured. Note that one-way ground-to-spacecraft signals are also possible, but present slightly different operational paradigms. Our analysis considers two- and one-way tracking as entirely separate cases; however there is no reason that these distinct types of tracking passes cannot be alternated throughout the course of a mission. The following discussion details some of the steps taken to model one-way Doppler and ranging tracking in our investigation.

One primary reason that one-way tracking is uncommon for deep-space applications is the need for precise timing information provided by an extremely accurate and stable on-board clock. Thus, two-way tracking has traditionally been favored due to the increased accuracy of ground-based atomic clocks and the relative availability of dedicated DSN tracking intervals. However, as the number of spacecraft operating across the solar system grows, there is additional pressure to be more efficient in the use of the DSN's limited resources. In turn, this has prompted the development of space-based atomic clocks appropriate for deep-space applications; the aptly named Deep Space Atomic Clock (DSAC) will soon be available for larger spacecraft[16] while Chip-Scale Atomic Clocks (CSACs) are currently being considered for SmallSats.[17] Ultra-stable oscillators (USOs) can provide the needed accuracy over intervals of 100s of seconds,[18] though gaps in tracking fail to capture random walks in the USO, leading to degraded navigation solutions.

Since two-way tracking has dominated deep-space navigation for the past several decades, comparatively little navigation software development has focused on supporting one-way measurement types. Indeed, only recently has MONTE begun to infuse precise on-board clock models and link them to the appropriate one-way measurement types so that accurate filtering simulations can be performed. Because of this relatively recent development history for the clock models, we have instead favored use of the more historical, and validated, spacecraft frequency models. While these frequency drift models may not be as precise as clock models, they are sufficiently accurate to support the covariance analyses presented in this investigation; we leave it as future work to fully validate the covariance assessments with more rigorous filtering simulations. For our analysis, we have transformed the performance specifications of the SA.45S Chip Scale Atomic Clock[17] into appropriate values for frequency stability, as shown in Table 1.

### II.iii Delta Differential One-Way Range Measurements

Delta Differential One-Way Ranging (DDOR) is commonly used to obtain precise plane-of-sky angular measurements to complement line-of-sight Doppler and range data. A spacecraft typically transmits special DOR tones which are received by two ground station antennas separated by a large geographic distance; for the analysis cases presented here, we alternate DDOR passes between Goldstone-Madrid and Goldstone-Canberra baselines. In fact, this alternation of baseline over a given tracking schedule is critical: if only one baseline is used, large state uncertainties can still remain in one axis lying in the plane-of-sky. Precise geometrical measurements of the spacecraft state are obtained by tracking the spacecraft range difference as measured by the two ground stations. Measurement errors due to atmospheric disturbances are eliminated by characterizing the atmospheric effects on a known quasar source. Because the measurement is the range difference observed by the two ground stations, on-board clock errors are differenced out, enabling precise measurements regardless of spacecraft frequency stability. In addition to the extra information from the alternative data type, one advantage to using DDOR is short tracking durations of 30-min to 1-hour; on the other hand, two antennas must be used, and DDOR passes can only occur where there are overlaps in coverage. Thus, the availability of DDOR is heavily dependent on DSN usage and the orbital geometry of the spacecraft in question. While we only consider the DSN-specific baselines, partner stations like those in Usuda, Japan or Malargüe, Argentina can also be used to form DDOR baselines with DSN stations, enabling some additional freedom in scheduling.

### II.iv Reference Spacecraft Trajectory

The baseline motion of our Earth-Moon analysis case is the lunar flyby trajectory pictured in Fig. 1, where the trajectory arc begins a few days after one

lunar flyby and targets a second close approach one month later. In this dynamical regime, the gravity of Earth and the Moon dominate and are represented with 8x8 and 50x50 spherical harmonics, respectively; solar gravity is included but modeled as a point-mass. Other perturbing effects may include solar radiation pressure (SRP) and unbalanced attitude control maneuvers; for our scenario, we assume a stochastic acceleration of $1.1 \times 10^{-12} km/sec^2$ in daily batches due to uncertainties in SRP (comparable to the value from the Mars Reconnaissance Orbiter cruise phase[19]) and weekly momentum desaturation maneuvers. A variety of mission concepts may

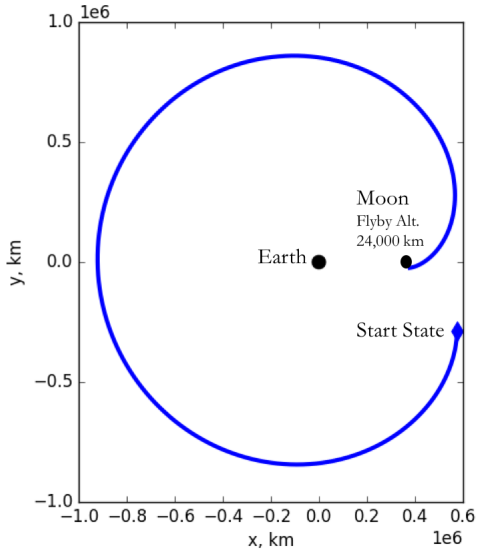


Fig. 1: Lunar flyby trajectory, shown in Earth-Moon rotating frame.

use such a lunar flyby arc or present similar operational considerations, including:

- libration point orbit (LPO) or distant retrograde orbit (DRO) architectures, for example relay missions;
- transport between these destination orbits; and
- low-energy escape from or return to the Earth-Moon region.

Some limited analogy can be made to lower-lunar orbits, though such comparisons should be used with caution. When operating in the Earth-Moon region, we can expect spacecraft to carry omni-directional antennas that have sufficient gain to be received on Earth. Thus, even body-fixed solar panels can remain sun-pointed while the spacecraft communicates with Earth, which will reduce the net negative drain on the SmallSat power system. However, battery sizing and thermal considerations may still limit the total transmitter "on" time and the frequency at which communication can be cycled. Likewise, since the moon presents an attractive target for many potential missions, we can expect plenty of opportunity for MSPA passes; on the other hand, the X-band beamwidth of the 34-meter DSN antennas is only 540 km at lunar distances (S-band is slightly better at 1830 km),[15] so hopes for continual MSPA usage may be overly optimistic.

## III. Doppler Only Tracking

This section presents a qualitative discussion of Doppler tracking performance in the Earth-Moon region. Two-way tracking uncertainties provide a standardized baseline, while one-way tracking results indicate the performance available from MSPA and other one-way scenarios. Tabulated results for these and all other cases are contained in the appendix.

### III.i Two-Way Doppler Tracking

We begin our discussion by focusing on the expected navigation performance available using two-way Doppler measurements, where these results serve as a useful baseline of comparison for other tracking scenarios. Furthermore, we can assess a minimal level of performance from DSN communications, as some amount of two-way communication is required for every mission. We run covariance analyses for a variety of weekly tracking schedules and tracking pass duration, namely:

- tracking 1, 2, 3, or 7 times a week; and,
- tracking pass durations of 30 minutes, 1, 2, 4, or 8 hours,

for a total set of 20 cases. Tables with summary results for state reconstruction and forward prediction specific to two-way Doppler tracking are contained in appendix; here we reproduce one table (Table 2) to illustrate and inform our discussion. All covariance values presented in this analysis are 1-$\sigma$ unless otherwise noted. For our purposes, "reconstruction" is defined to mean the ability to bound the state at the epoch of data cut-offs (DCOs). for the last tracking pass. For this case, "prediction" is the estimation of a state six weeks after DCO. As is expected, navigation performance improves with more frequent tracking and longer passes. However, securing longer continuous tracking passes, if they can be supported by the

Table 2: Two-way Doppler-only position reconstruction accuracy at data cut-off. Approximate values of the principal axes of the uncertainty ellipsoid, in km.

| **Passes / Week** | **Pass Duration** | | | | |
|---|---|---|---|---|---|
| | 30 min. | 1 hr. | 2 hrs. | 4 hrs. | 8 hrs. |
| 1 | (54.93, 18.1, 6.89) | (14.58, 10.43, 2.6) | (13.09, 1.91, 1.02) | (12.43, 0.57, 0.36) | (3.67, 0.47, 0.09) |
| 2 | (37.85, 7.06, 4.02) | (7.91, 3.6, 1.66) | (1.81, 1.05, 0.57) | (0.41, 0.34, 0.27) | (0.27, 0.23, 0.08) |
| 3 | (7.22, 4.06, 1.19) | (4.77, 1.89, 1.01) | (1.41, 0.82, 0.43) | (0.35, 0.27, 0.22) | (0.22, 0.19, 0.05) |
| 7 | (2.56, 2.07, 0.72) | (2.18, 1.08, 0.59) | (0.93, 0.58, 0.31) | (0.28, 0.21, 0.19) | (0.17, 0.12, 0.05) |

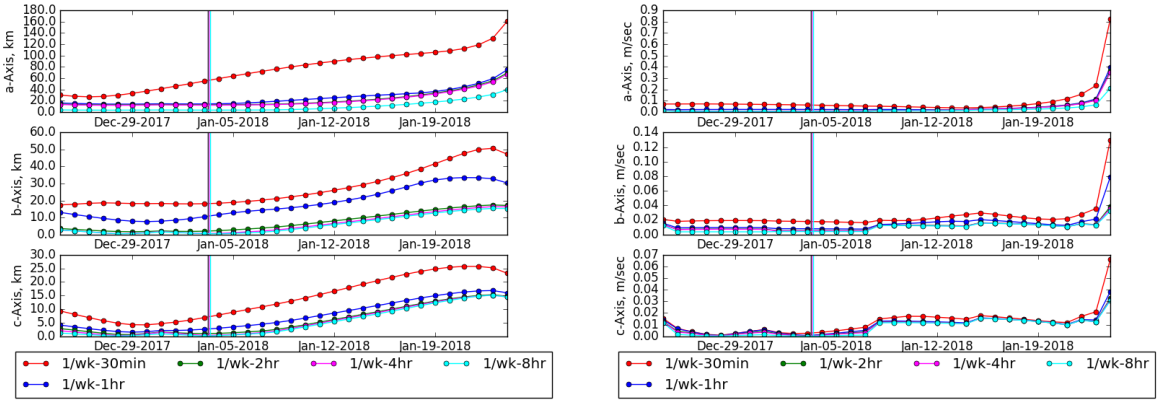


(a)*Position* (b)*Velocity*

Fig. 2: Growth in position and velocity uncertainty for 2-way Doppler only, 1 pass per week. Vertical lines are data cut-offs (DCOs).

spacecraft, seems to be a more effective strategy than increasing the number of passes; note, for example, that one weekly pass of 8 hours is comparable in both reconstructive and predictive power to daily passes of 2 to 4 hours. Note also the apparent law of diminishing marginal utility (a phrase we freely borrow from economics): at some point increases in pass frequency and duration provide only modest improvements in uncertainty, at least in terms of absolute values.

Some notable aspects of the state uncertainty time history are not captured by the simple quantitative comparison presented so far. Thus, we turn to an assessment of the evolution of the covariance ellipsoids over time. Figure 2 illustrates the time history of the principal components of the 3-D position and velocity uncertainty ellipsoids for one pass per week; the $a$-, $b$-, and $c$-axes are the major, intermediate, and minor principal axes of the uncertainty ellipsoid, respectively. Note that for tracking durations of less than 1 hour, the major and intermediate axes of the position covariance grow from the initial epoch of the simulation, through DCO, and on to the end of the prediction interval. Likewise, velocity covariances are degraded for these cases as well. By implication, the estimates of other spacecraft parameters such as maneuver execution and solar radiation pressure (SRP) would be equally suspect. It is worth noting, though, that even relatively short two-way tracking passes may be sufficient for reconstructing the state and other spacecraft parameters for many mission scenarios, and some negative effects of sub-hour tracking can be removed by the addition of one extra tracking pass per week. As we show in Fig. 3, increasing the number of tracking passes removes pre-DCO kinks in the velocity reconstruction, indicating that additional components of the maneuver performance are resolved. In contrast, the qualitative behavior of the largest principal axis does not change, even if tracking is increased to a daily occurrence. This observation reinforces two common rules of thumb in deep-space navigation:

1. Keep tracking passes sufficiently long in order to:
   (a) resolve stochastic or bias effects of long-term perturbations like SRP or gravity mismodeling; and,

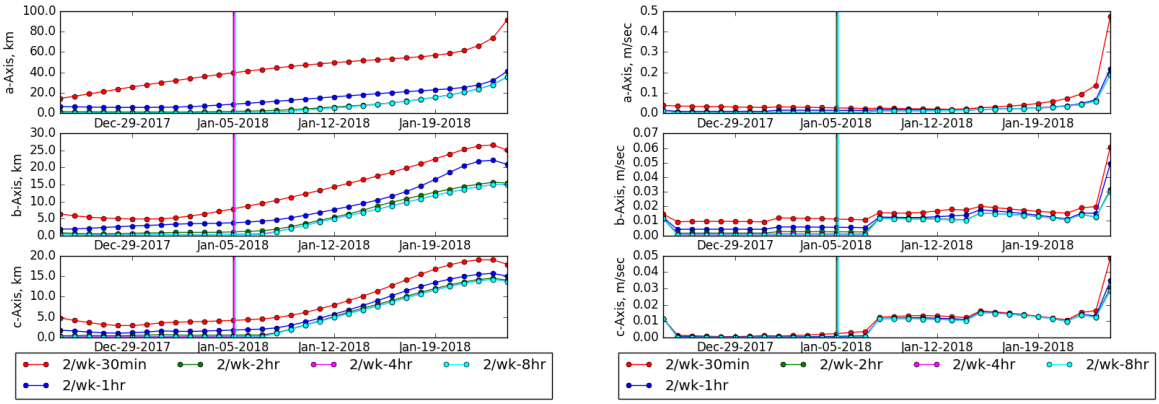


(a)*Position* (b)*Velocity*

Fig. 3: Growth in position and velocity uncertainty for 2-way Doppler only, 2 passes per week. Vertical lines are data cut-offs (DCOs).

(b) ascertain right ascension and declination information from the Earth's rotational signature (Hamilton-Melbourne Theory).[13]

2. Budget $n + 1$ tracking passes for every $n$ maneuvers in order to characterize thruster performance, -or- perform maneuvers in the middle of longer tracking passes.

While Figs. 2 and 3 highlight the behavior of the principal axes of the covariance ellipsoid, a common navigation practice is to view these values as projections onto some invariant plane, commonly the B-plane of a target body. Thus, we present notional B-plane ellipses in Fig. 4; since we are not estimating state updates via a filtering process, we center the uncertainty ellipses on (0,0). Note the different alignments of the uncertainty ellipses for the 30-min tracking scenario versus the longer pass durations. Note also that weekly 1-, 2-, and 4-hour passes are roughly equivalent in predictive power, while 8-hour passes provide significantly improved estimates in the largest principal axis.

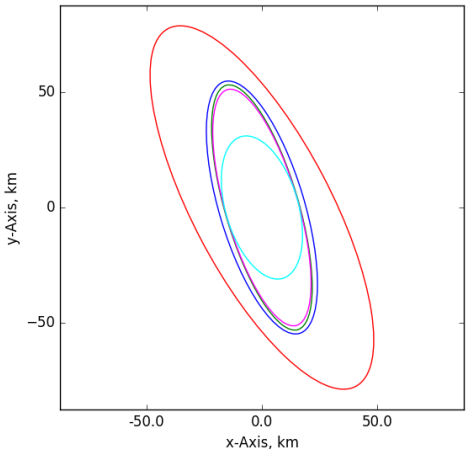


Fig. 4: B-plane uncertainty ellipses for 2-way Doppler only, 1 pass per week. Color matches key from Fig. 2.

III.ii One-Way Doppler Tracking

We turn now to the one-way Doppler measurement type, where we begin our analysis by considering one-way Doppler measurements as the sole information source for state estimation (note our assumed use of a CSAC for precise timing). In reality, some two-way communication may be intermixed with the one-way passes; however, we neglect this consideration in favor of the more conservative one-way only scenario. As with two-way tracking, we run cases for 1,

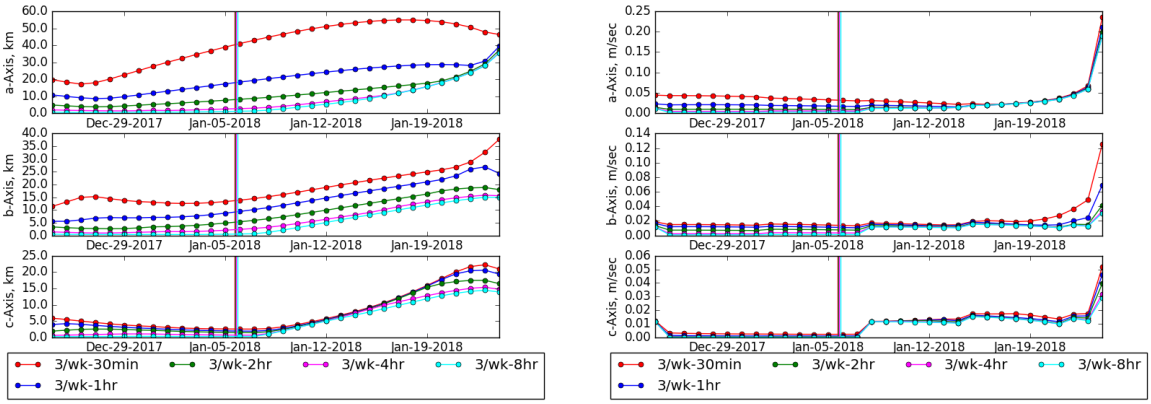


(a)*Position* (b)*Velocity*

Fig. 5: Growth in position and velocity uncertainty for 1-way Doppler only, 3 passes per week. Vertical lines are data cut-offs (DCOs).

2, 3, and 7 passes per week and 30-min, 1-, 2-, 4-, 8-hour durations. Overall, the same general trends emerge for one-way as for two-way tracking, though with uncertainties 2-4 times larger than for pure two-way tracking: longer durations are more beneficial than multiple passes and the marginal utility of additional tracking quickly drops off. However, the time-history behavior of the covariances shows remarkable degradation, as is evidenced by Figs. 5 and 6. Even for thrice-weekly passes, state uncertainties prior to DCO do not have consistent magnitudes over time, with correspondingly large uncertainties in other operational parameters. It is only with daily tracking passes that reconstructions in the $XY$-plane achieve a steady level; as with two-way tracking, passes of 2 or more hours are highly desirable to reduce uncertainties.

## IV. Additional Measurement Types

We now consider the use of supplemental measurement types in conjunction with, or in place of, traditional Doppler measurements. In particular, we focus on ranging, either via single-antenna methods or through the use of DDOR.

### IV.i Range Data Types

We first consider traditional ranging schemes which can be performed simultaneously with Doppler measurements. As can be seen for two-way SRA in Fig. 7, the performances in Doppler-only and ranging-only are similar in magnitude, if not exact qualitative behavior. However, when the measurements types

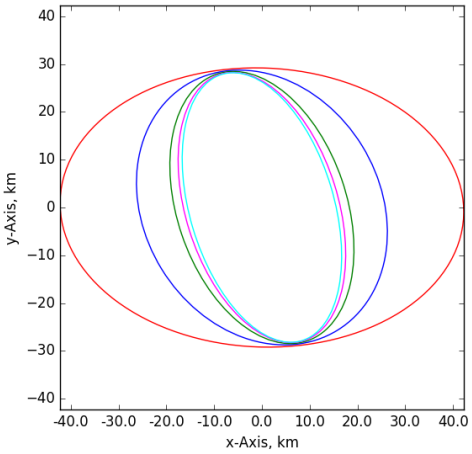


Fig. 6: B-plane uncertainty ellipses for 1-way Doppler only, 3 passes per week. Color matches key from Fig. 5.

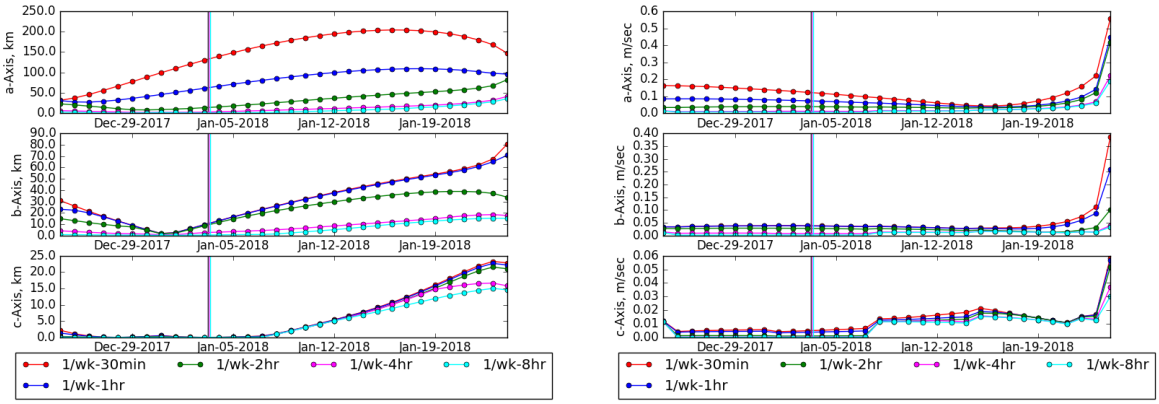


(a)*Position* (b)*Velocity*

Fig. 7: Growth in position and velocity uncertainty for 2-way SRA, 1 pass per week. Vertical lines are data cut-offs (DCOs).

are considered simultaneously, as in Fig. 8, the performance is significantly improved for tracking passes of less than 1 hour. On the other hand, two-way ranging has the potential to degrade telemetry, so its use cannot always be assumed for all cases. One-way ranging has a similar performance boosting capability when used in conjunction with one-way Doppler, though we caution the reader that the combined simulation results should be treated especially cautiously, given the previously mentioned modeling limitations.

### IV.ii Delta Differential One-way Range

We now consider the addition of DDOR data in the two- and one-way tracking scenarios discussed previously. Specifically, we include either monthly or weekly DDOR tracking passes interspersed within the already established Doppler schedules. The following discussion focuses on these two cases and their implications for deep-space navigation; for this analysis, DDOR tracking passes are assumed to be 30 minutes in duration.

The inclusion of monthly DDOR passes into sparse tracking schedules dramatically decreases state uncertainty, as can be seen when comparing the covariance values for two-way Doppler in Table 3 to those in Table 2. In particular, note that one DDOR pass per month combined with once-per-week, 30-min, two-Way Doppler passes produces reconstructed and predicted uncertainties comparable to thrice weekly passes of 30-min duration or weekly passes of 1-2 hours. The effects are even more dramatic when DDOR is used in conjunction with one-way Doppler tracking, where this combination produces navigation uncertainties well below that of purely two-way tracking.

An examination of the covariance time histories reveals an equally impressive change in qualitative behavior when DDOR tracking is included every month. Figures 9 and 10 illustrate the growth in uncertainty for two- and one-way Doppler tracking in conjunction with monthly DDOR. In both cases, the growth in uncertainty of the reconstructed states is delayed by the inclusion of monthly DDOR measurements. However, the growth prior to DCO is not entirely eliminated for short tracking passes; passes of at least one hour are required for consistent state reconstruction. Note also the "pinching" in the covariances at the epochs of the DDOR passes; the most accurate reconstructions will understandably be for epochs when the most precise measurements are available.

Weekly DDOR tracking further decreases state covariances, though the qualitative differences between weekly and monthly DDOR are slight. Daily passes are still required for one-way Doppler tracking to provide consistent state reconstructions; in contrast, weekly DDOR tracking enables even weekly two-way Doppler passes to provide consistent reconstructions, regardless of pass duration.

## V. Conclusions

Efficient use of the tracking and telecommunications capability of the Deep Space Network is an increasing concern, especially given the predicted growth in the number of deep space missions. In particular, SmallSat missions with constrained bud-

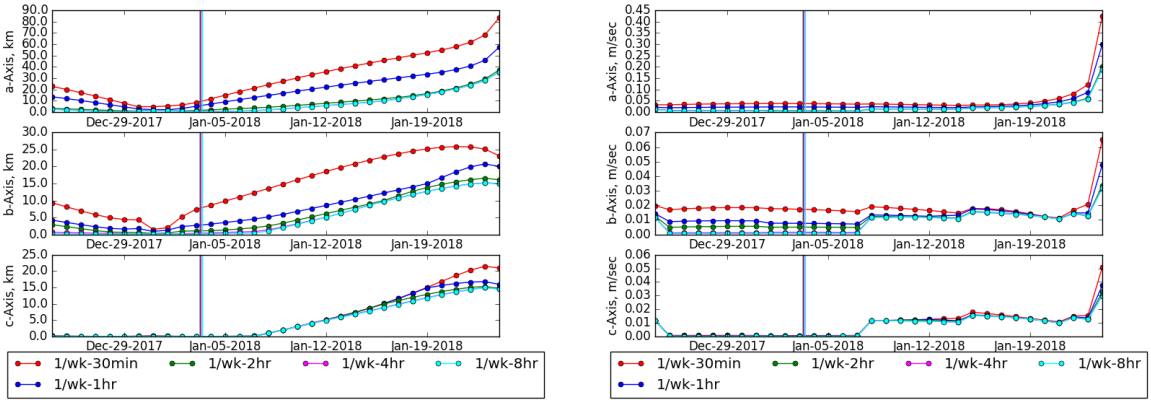


(a)*Position* (b)*Velocity*

Fig. 8: Growth in position and velocity uncertainty for 2-way Doppler plus SRA, 1 pass per week. Vertical lines are data cut-offs (DCOs).

Table 3: Two-way Doppler plus monthly DDOR position reconstruction accuracy at data cut-off. Approximate values of the principal axes of the uncertainty ellipsoid, in km.

| **Passes Per Week** | **Pass Duration** | | | | |
|---|---|---|---|---|---|
| | 30 min. | 1 hr. | 2 hrs. | 4 hrs. | 8 hrs. |
| 1 | (18.25, 11.58, 6.06) | (13.58, 6.05, 2.6) | (8.12, 1.67, 1.0) | (6.78, 0.55, 0.33) | (2.71, 0.36, 0.07) |
| 2 | (9.0, 6.97, 0.45) | (5.67, 2.5, 0.43) | (1.63, 1.01, 0.42) | (0.41, 0.33, 0.27) | (0.26, 0.21, 0.08) |
| 3 | (4.49, 2.65, 0.38) | (3.02, 1.87, 0.36) | (1.19, 0.81, 0.33) | (0.35, 0.26, 0.22) | (0.22, 0.18, 0.05) |
| 7 | (2.46, 1.65, 0.33) | (2.11, 1.07, 0.32) | (0.9, 0.58, 0.28) | (0.27, 0.21, 0.19) | (0.17, 0.12, 0.05) |

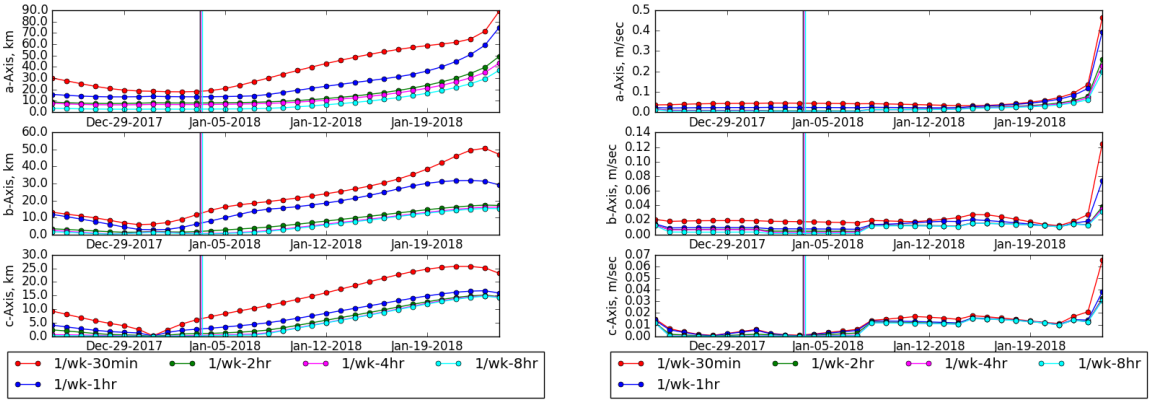


(a)*Position* (b)*Velocity*

Fig. 9: Growth in position and velocity uncertainty for 2-way Doppler plus DDOR: 1 Doppler pass per week, 1 DDOR pass per month. Vertical lines are data cut-offs (DCOs).

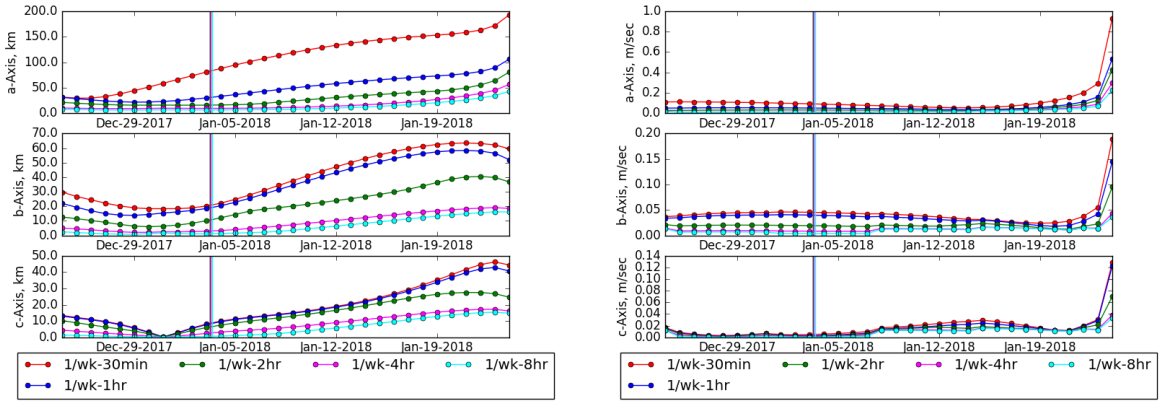


(a)*Position* (b)*Velocity*

Fig. 10: Growth in position and velocity uncertainty for 1-way Doppler plus DDOR: 1 Doppler pass per week, 1 DDOR pass per month. Vertical lines are data cut-offs (DCOs).

gets will need to be parsimonious in DSN usage and will need to carefully calibrate mission objectives and requirements to match available DSN support. As demonstrated throughout this investigation, precise state estimation relies on plentiful and accurate measurement data, whether that information is from traditional two-way tracking or alternative data sources. Note that we have not considered relative navigation, whether for formations of spacecraft or for exploration of primitive bodies; inter-spacecraft ranging, optical navigation, or differential measurements may be required for applications where precise knowledge of relative states is required. However, we present a catalogue of DSN tracking scenarios for lunar mission architectures that planners can use to inform their initial trade studies. Qualitative results are summarized as follows:

1. Long duration Doppler passes enable precise navigation:
   (a) Two-way Doppler tracking, the most commonly used DSN measurement type, provides the baseline for comparison;
   (b) One-way Doppler measurements exploit the forthcoming multiple spacecraft tracking capability of the DSN, but rely on precise clocks; even so, accuracy is generally an order of magnitude worse than two-way tracking;
   (c) Sparse tracking with short passes can meet loose positioning requirements, but with degraded capability to reconstruct the spacecraft state and other operational parameters;
2. Ranging measurements, including DDOR, provide a complementary capability that:
   (a) Greatly improves navigation accuracies, though the effect is most pronounced for short and sparse Doppler passes;
   (b) Enables reconstruction of additional spacecraft parameters when short Doppler passes are used;
   (c) For DDOR, requires the use of two DSN antennas, though less frequently and for shorter intervals than Doppler measurements.

Tabulated results for different tracking schedules and mission architectures can be found in the appendix and are provided as a reference for mission planners. Note that these are just guidelines; selection of the proper schedule and measurement types will be mission dependent, especially since hardware limitations may necessitate short tracking passes. But, a variety of tracking options can provide comparable navigational accuracies, so most missions should be able to find an option that satisfies their specific needs while still enabling efficient use of limited DSN resources.

In general, we expect state reconstructions based on Doppler data to be more precise when near massive gravitating bodies, even if forward predictions may become less certain. Briefly, Doppler provides a direct measurement of relative velocity and, therefore, we gain more insight into the current mo-

tion of the spacecraft when velocity changes are more pronounced. For lunar region applications, reconstructed position uncertainties can range from roughly 100 km for the most sparse one-way tracking scenarios, to sub-kilometer accuracies for extensive two-way tracking. Likewise, forward prediction accuracies range from roughly 300 km down to single digit kilometers. Note that sparse one-way tracking schemes do raise concerns about acquiring contact with the DSN: the $1-\sigma$ uncertainties in position are of the same order of magnitude as the X-band beam width of the 34-m antennas. However, given the projected number of missions to the lunar region within the next decade, opportunities for MSPA are expected to be relatively frequent, which in turn indicates that a significant number of smallsat missions could rely on one-way measurements as a major component of their navigation plan. In particular, routine operations in LPOs and DROs could be fully supported by a mix of one-way and two-way Doppler tracking (note again that we speak in terms of absolute knowledge, not relative navigation within a formation or constellation). Inclusion of ranging and/or DDOR has notable positive effects on navigation estimates, but the best use of DDOR may remain to provide supplementary tracking for already sparse schedules to support close approaches to the Moon or Earth, for example on transfer, escape, or capture trajectories. Although we focused on a lunar flyby trajectory, our investigation could inform tracking analysis for lunar-centric orbits, though we caution the reader to use his or her own judgement when applying our conclusions to these different cases; our results may well apply to high-altitude orbits above the moon, but low-lunar orbits require separate consideration.

While this investigation comprehensively analyzed the navigation performance of Doppler and DDOR measurement types in straight-forward tracking schedules, some avenues for future work remain. First, sample cases showing the effects of intermixing two- and one-way measurements would provide more realistic uncertainties for some possible operational paradigms. Additionally, fitting multiple 30-min segments into longer 4- or 8-hour tracking passes may provide a more accurate simulation of MSPA operation, and could provide a significant portion of the geometric information contained in a continuous long-duration pass. Finally, accurate modeling of clock behavior and performance will increase the fidelity of one-way measurement simulations, providing a more accurate assessment of potential navigation performance.

## VI. Acknowledgements

This research was carried out at the Jet Propulsion Laboratory, California Institute of Technology, under a contract with the National Aeronautics and Space Administration.

## VII. Appendix - Tabulated Data

*NOTE:* All covariance values presented in this analysis are 1-$\sigma$ unless otherwise noted. The approximate values presented here represent a specific analysis case of lunar transport and should ONLY be used to estimate orders of magnitude more generally. As always, the best course of action is to conduct your own analysis for your specific use case. All one-way measurement type results tabulated here assume the use of a Chip-Scale Atomic Clock[17] that is currently being evaluated for future use on SmallSats; currently available clocks suitable for SmallSat applications are much less precise.

## References

[1] California Polytechnic State University, "CubeSat Design Specification, $13^{th}$ Ed.," February 20, 2014, `http://www.cubesat.org/resources/`

[2] S. Asmar and S. Matousek, "Mars Cube One (MarCO) - The First Planetary CubeSat Mission," *Mars CubeSat / NanoSat Workshop*, Pasadena, California, November 20-21, 2014

[3] A. Klesh, et al., "INSPIRE: Interplanetary NanoSpacecraft Pathfinder In Relevant Environment," *Proceedings of the $27^{th}$ Annual AIAA/USU Conference on Small Satellites*, Logan, Utah, August, 2013, Paper No. SSC13-XI-8

[4] P. Hayne, et al., "Lunar Flashlight: Illuminating the Moon's South Pole," *Proceedings of the $47^{th}$ Lunar and Planetary Science Conference*, Houston, Texas, March 22-25, 2016

[5] J. Castillo-Rogez, et al., "Near Earth Asteroid Scout Mission," $11^{th}$ *Meeting of the NASA Small Bodies Assessment Group (SBAG)*, Washington, D.C., July 29-31, 2015

[6] L. Wood, "The Evolution of Deep Space Navigation: 1962-1989," *Advances in the Astronautical Sciences*, Vol. 131, 2008, pg. 285-308

[7] L. Wood, "The Evolution of Deep Space Navigation: 1989-1999," *Advances in the Astronautical Sciences*, Vol. 132, 2008, pg. 877-898

[8] L. Wood, "The Evolution of Deep Space Navigation: 1999-2004," *Advances in the Astronautical Sciences*, Vol. 152, 2014, pg. 827-847

[9] L. Wood, "The Evolution of Deep Space Navigation: 2004-2006," *Advances in the Astronautical Sciences*, Vol. 160, 2017, pg. 3271-3292

Table 4: Two-way Doppler-only position reconstruction accuracy at data cut-off. Approximate values of the principal axes of the uncertainty ellipsoid, in km.

| **Passes** | **Pass Duration** | | | | |
|---|---|---|---|---|---|
| **Per Week** | 30 min. | 1 hr. | 2 hrs. | 4 hrs. | 8 hrs. |
| 1 | (54.93, 18.1, 6.89) | (14.58, 10.43, 2.6) | (13.09, 1.91, 1.02) | (12.43, 0.57, 0.36) | (3.67, 0.47, 0.09) |
| 2 | (37.85, 7.06, 4.02) | (7.91, 3.6, 1.66) | (1.81, 1.05, 0.57) | (0.41, 0.34, 0.27) | (0.27, 0.23, 0.08) |
| 3 | (7.22, 4.06, 1.19) | (4.77, 1.89, 1.01) | (1.41, 0.82, 0.43) | (0.35, 0.27, 0.22) | (0.22, 0.19, 0.05) |
| 7 | (2.56, 2.07, 0.72) | (2.18, 1.08, 0.59) | (0.93, 0.58, 0.31) | (0.28, 0.21, 0.19) | (0.17, 0.12, 0.05) |

[10] B. Tapley, B. Schutz, and G. Born, *Statistical Orbit Determination*, Elsevier, Inc., Burlington, Massachusetts, 2004

[11] S. Evans, et al. "MONTE: The Next Generation of Mission Design & Navigation Software," *The* $6^{th}$ *International Conference on Astrodynamics Tools and Techniques (ICATT)*, Darmstadt, Germany, March 14-17, 2016, `https://indico.esa.int/indico/event/111/session/30/contribution/177`

[12] Solar System Dynamics Group, "HORIZONS System," Jet Propulsion Laboratory, California Institute of Technology, `http://ssd.jpl.nasa.gov/?horizons`

[13] T. Hamilton and W. Melbourne, "Information Content of a Single Pass of Doppler Data from a Distant Spacecraft," Jet Propulsion Laboratory, California Institute of Technology, May 31, 1966, pg. 18-23, Report No. JPL-SPS 37-39, `http://descanso.jpl.nasa.gov/history/DSNTechRefs.html`

[14] T. Moyer, *Formulation for Observed and Computed Values of Deep Space Network Data Types for Navigation*, John Wiley & Sons, Inc., Hoboken, New Jersey, 2003

[15] Deep Space Network Project Office, *DSN Telecommunications Link Design Handbook*, Jet Propulsion Laboratory, California Institute of Technology, Document 810-005, `http://deepspace.jpl.nasa.gov/dsndocs/810-005/`

[16] T. Ely and J. Seubert, "One-Way Radiometric Navigation with the Deep Space Atomic Clock," *Advances in the Astronautical Sciences*, Vol. 155, 2015, pg. 2799-2816

[17] R. Lutwak, "The SA.45S Chip-Scale Atomic Clock," *2011 Stanford PNT Symposium*, Menlo Park, California, November 17-18, 2011

[18] S. Asmar, "Ultra-Stable Oscillators for Probe Radio Science Investigations," $9^{th}$ *International Planetary Probe Workshop*, Toulouse, France, June 16-17, 2012

[19] T.-H. You, et al. "Navigating Mars Reconnaissance Orbiter: Launch Through Primary Science Orbit," *AIAA SPACE 2007 Conference & Exposition*, Long Beach, California, September 18-20, 2007, AIAA Paper 2007-6093

Table 5: Two-way Doppler-only velocity reconstruction accuracy at data cut-off. Approximate values of the principal axes of the uncertainty ellipsoid, in mm/sec.

| **Passes** | **Pass Duration** | | | | |
|---|---|---|---|---|---|
| **Per Week** | 30 min. | 1 hr. | 2 hrs. | 4 hrs. | 8 hrs. |
| 1 | (63.33, 17.82, 2.61) | (23.96, 7.79, 0.71) | (8.79, 5.25, 0.2) | (7.49, 4.83, 0.1) | (4.79, 3.97, 0.04) |
| 2 | (27.35, 11.52, 1.82) | (14.33, 5.7, 0.53) | (3.93, 2.51, 0.13) | (1.25, 1.02, 0.03) | (0.84, 0.3, 0.02) |
| 3 | (8.21, 6.88, 0.42) | (6.32, 4.55, 0.26) | (2.87, 2.0, 0.1) | (1.0, 0.83, 0.05) | (0.68, 0.23, 0.03) |
| 7 | (3.87, 2.24, 0.24) | (3.24, 1.64, 0.15) | (1.51, 0.98, 0.07) | (0.53, 0.49, 0.03) | (0.29, 0.2, 0.02) |

Table 6: Two-way Doppler-only position prediction accuracy at lunar close approach. Approximate values of the principal axes of the uncertainty ellipsoid, in km.

| **Passes** | **Pass Duration** | | | | |
|---|---|---|---|---|---|
| **Per Week** | 30 min. | 1 hr. | 2 hrs. | 4 hrs. | 8 hrs. |
| 1 | (160.8, 47.3, 23.2) | (75.0, 30.3, 16.0) | (69.4, 17.1, 14.7) | (66.8, 16.2, 14.5) | (39.8, 15.3, 14.5) |
| 2 | (91.9, 25.1, 17.9) | (41.0, 20.9, 15.0) | (35.7, 15.4, 14.0) | (35.4, 14.9, 13.7) | (35.4, 14.9, 13.7) |
| 3 | (36.7, 17.2, 16.1) | (36.2, 16.5, 14.6) | (35.5, 15.2, 13.9) | (35.4, 14.9, 13.7) | (35.4, 14.9, 13.7) |
| 7 | (21.6, 13.8, 11.0) | (21.4, 13.2, 10.9) | (20.5, 11.4, 10.7) | (17.1, 10.0, 9.3) | (15.2, 9.1, 8.6) |

Table 7: Two-way Doppler-only velocity prediction accuracy at lunar close approach. Approximate values of the principal axes of the uncertainty ellipsoid, in mm/sec.

| **Passes** | **Pass Duration** | | | | |
|---|---|---|---|---|---|
| **Per Week** | 30 min. | 1 hr. | 2 hrs. | 4 hrs. | 8 hrs. |
| 1 | (823.1, 129.8, 66.0) | (394.7, 79.0, 38.5) | (363.1, 38.1, 32.7) | (350.0, 35.4, 31.7) | (211.8, 32.2, 30.6) |
| 2 | (474.2, 60.9, 48.5) | (218.0, 49.3, 34.7) | (190.8, 31.6, 30.4) | (189.3, 30.3, 28.8) | (189.1, 30.2, 28.7) |
| 3 | (196.7, 40.2, 36.7) | (194.0, 35.7, 32.6) | (189.8, 30.9, 29.7) | (189.2, 30.3, 28.8) | (189.1, 30.2, 28.7) |
| 7 | (113.3, 29.8, 22.3) | (112.5, 27.8, 21.8) | (109.3, 22.4, 20.6) | (95.0, 17.5, 16.3) | (85.8, 15.3, 12.9) |

Table 8: Two-way SRA-only position reconstruction accuracy at data cut-off. Approximate values of the principal axes of the uncertainty ellipsoid, in km.

| **Passes** | **Pass Duration** | | | | |
|---|---|---|---|---|---|
| **Per Week** | 30 min. | 1 hr. | 2 hrs. | 4 hrs. | 8 hrs. |
| 1 | (130.02, 9.6, 0.01) | (61.2, 9.47, 0.0) | (13.47, 8.47, 0.0) | (2.66, 2.5, 0.0) | (0.67, 0.35, 0.0) |
| 2 | (11.13, 0.98, 0.02) | (7.22, 0.35, 0.01) | (4.52, 0.22, 0.0) | (1.43, 0.18, 0.0) | (0.5, 0.16, 0.0) |
| 3 | (4.37, 0.76, 0.0) | (1.81, 0.33, 0.0) | (0.93, 0.15, 0.0) | (0.7, 0.1, 0.0) | (0.39, 0.08, 0.0) |
| 7 | (0.45, 0.15, 0.0) | (0.21, 0.13, 0.0) | (0.11, 0.08, 0.0) | (0.07, 0.03, 0.0) | (0.03, 0.02, 0.0) |

Table 9: Two-way SRA-only velocity reconstruction accuracy at data cut-off. Approximate values of the principal axes of the uncertainty ellipsoid, in mm/sec.

| **Passes** | **Pass Duration** | | | | |
|---|---|---|---|---|---|
| **Per Week** | 30 min. | 1 hr. | 2 hrs. | 4 hrs. | 8 hrs. |
| 1 | (122.82, 38.27, 4.86) | (72.89, 37.5, 3.72) | (38.62, 27.66, 0.99) | (11.29, 7.46, 0.27) | (5.0, 1.57, 0.06) |
| 2 | (9.54, 2.83, 1.21) | (5.55, 1.59, 0.53) | (3.83, 1.02, 0.25) | (2.79, 0.63, 0.1) | (1.45, 0.51, 0.03) |
| 3 | (5.72, 2.7, 0.17) | (3.36, 1.11, 0.08) | (2.05, 0.59, 0.06) | (1.73, 0.4, 0.05) | (1.15, 0.32, 0.04) |
| 7 | (0.69, 0.34, 0.14) | (0.47, 0.31, 0.1) | (0.31, 0.23, 0.07) | (0.23, 0.17, 0.06) | (0.17, 0.14, 0.03) |

 

Table 10: Two-way SRA-only position prediction accuracy at lunar close approach. Approximate values of the principal axes of the uncertainty ellipsoid, in km.

| **Passes** | **Pass Duration** | | | | |
|---|---|---|---|---|---|
| **Per Week** | 30 min. | 1 hr. | 2 hrs. | 4 hrs. | 8 hrs. |
| 1 | (147.2, 80.7, 22.8) | (95.9, 70.8, 22.2) | (82.1, 33.8, 21.0) | (41.1, 17.6, 15.8) | (35.5, 15.0, 14.6) |
| 2 | (35.9, 17.1, 14.9) | (35.5, 15.4, 14.6) | (35.4, 15.0, 14.3) | (35.4, 15.0, 13.9) | (35.4, 14.9, 13.7) |
| 3 | (35.6, 15.6, 14.7) | (35.4, 15.0, 14.0) | (35.4, 15.0, 13.8) | (35.4, 14.9, 13.7) | (35.4, 14.9, 13.7) |
| 7 | (20.9, 13.6, 10.7) | (20.8, 13.2, 10.7) | (20.7, 12.7, 10.7) | (20.6, 11.6, 10.6) | (16.8, 9.9, 9.6) |

Table 11: Two-way SRA-only velocity prediction accuracy at lunar close approach. Approximate values of the principal axes of the uncertainty ellipsoid, in mm/sec.

| **Passes** | **Pass Duration** | | | | |
|---|---|---|---|---|---|
| **Per Week** | 30 min. | 1 hr. | 2 hrs. | 4 hrs. | 8 hrs. |
| 1 | (556.3, 385.7, 58.5) | (447.8, 258.8, 56.5) | (415.9, 100.9, 51.7) | (219.9, 38.8, 37.0) | (189.7, 32.2, 30.0) |
| 2 | (192.7, 42.6, 30.2) | (189.8, 36.6, 29.6) | (189.3, 33.2, 29.4) | (189.2, 31.0, 29.1) | (189.1, 30.3, 28.8) |
| 3 | (190.4, 35.0, 30.2) | (189.3, 31.4, 29.3) | (189.2, 30.6, 28.9) | (189.1, 30.5, 28.8) | (189.1, 30.3, 28.7) |
| 7 | (110.5, 28.7, 20.8) | (110.4, 27.7, 20.7) | (110.3, 26.0, 20.6) | (109.8, 23.1, 20.4) | (93.4, 17.6, 16.7) |

Table 12: Two-way Doppler+SRA position reconstruction accuracy at data cut-off. Approximate values of the principal axes of the uncertainty ellipsoid, in km.

| **Passes** | **Pass Duration** | | | | |
|---|---|---|---|---|---|
| **Per Week** | 30 min. | 1 hr. | 2 hrs. | 4 hrs. | 8 hrs. |
| 1 | (8.55, 7.43, 0.0) | (5.24, 2.65, 0.0) | (1.54, 1.04, 0.0) | (0.59, 0.32, 0.0) | (0.48, 0.06, 0.0) |
| 2 | (2.77, 0.14, 0.0) | (1.29, 0.13, 0.0) | (0.81, 0.17, 0.0) | (0.38, 0.15, 0.0) | (0.21, 0.07, 0.0) |
| 3 | (0.72, 0.09, 0.0) | (0.68, 0.09, 0.0) | (0.54, 0.08, 0.0) | (0.32, 0.07, 0.0) | (0.21, 0.04, 0.0) |
| 7 | (0.07, 0.04, 0.0) | (0.06, 0.03, 0.0) | (0.04, 0.02, 0.0) | (0.03, 0.02, 0.0) | (0.02, 0.01, 0.0) |

Table 13: Two-way Doppler+SRA velocity reconstruction accuracy at data cut-off. Approximate values of the principal axes of the uncertainty ellipsoid, in mm/sec.

| **Passes** | **Pass Duration** | | | | |
|---|---|---|---|---|---|
| **Per Week** | 30 min. | 1 hr. | 2 hrs. | 4 hrs. | 8 hrs. |
| 1 | (37.99, 17.3, 0.58) | (23.12, 7.64, 0.28) | (6.69, 5.02, 0.13) | (4.88, 1.49, 0.05) | (4.76, 0.72, 0.02) |
| 2 | (3.27, 0.79, 0.21) | (2.81, 0.62, 0.12) | (2.08, 0.56, 0.05) | (1.17, 0.47, 0.03) | (0.7, 0.25, 0.02) |
| 3 | (1.78, 0.4, 0.05) | (1.71, 0.37, 0.05) | (1.48, 0.34, 0.04) | (0.96, 0.29, 0.04) | (0.66, 0.19, 0.02) |
| 7 | (0.23, 0.18, 0.05) | (0.21, 0.16, 0.05) | (0.19, 0.15, 0.03) | (0.17, 0.14, 0.02) | (0.15, 0.13, 0.01) |

Table 14: Two-way Doppler+SRA position prediction accuracy at lunar close approach. Approximate values of the principal axes of the uncertainty ellipsoid, in km.

| **Passes** | **Pass Duration** | | | | |
|---|---|---|---|---|---|
| **Per Week** | 30 min. | 1 hr. | 2 hrs. | 4 hrs. | 8 hrs. |
| 1 | (83.5, 23.1, 21.0) | (57.5, 20.0, 15.9) | (37.4, 16.1, 14.7) | (35.5, 15.0, 14.5) | (35.4, 14.9, 14.5) |
| 2 | (35.4, 15.0, 14.1) | (35.4, 15.0, 13.9) | (35.4, 14.9, 13.8) | (35.4, 14.9, 13.7) | (35.4, 14.9, 13.7) |
| 3 | (35.4, 14.9, 13.8) | (35.4, 14.9, 13.7) | (35.4, 14.9, 13.7) | (35.4, 14.9, 13.7) | (35.4, 14.9, 13.7) |
| 7 | (20.6, 11.6, 10.5) | (20.6, 11.3, 10.3) | (20.1, 10.9, 9.9) | (16.7, 9.9, 9.2) | (15.1, 9.0, 8.5) |

Table 15: Two-way Doppler+SRA velocity prediction accuracy at lunar close approach. Approximate values of the principal axes of the uncertainty ellipsoid, in mm/sec.

| **Passes** | **Pass Duration** | | | | |
|---|---|---|---|---|---|
| **Per Week** | 30 min. | 1 hr. | 2 hrs. | 4 hrs. | 8 hrs. |
| 1 | (424.8, 65.1, 51.0) | (299.5, 47.9, 37.4) | (200.1, 33.6, 32.6) | (189.6, 32.0, 29.9) | (189.2, 31.9, 29.7) |
| 2 | (189.2, 31.8, 29.2) | (189.2, 31.0, 29.1) | (189.1, 30.6, 28.9) | (189.1, 30.3, 28.8) | (189.1, 30.2, 28.7) |
| 3 | (189.1, 30.5, 28.8) | (189.1, 30.5, 28.8) | (189.1, 30.4, 28.8) | (189.1, 30.2, 28.7) | (189.0, 30.2, 28.7) |
| 7 | (109.9, 23.2, 20.1) | (109.7, 22.1, 19.5) | (107.9, 20.8, 18.2) | (93.2, 17.0, 15.7) | (85.6, 15.0, 12.8) |

Table 16: Two-way Doppler plus monthly DDOR position reconstruction accuracy at data cut-off. Approximate values of the principal axes of the uncertainty ellipsoid, in km.

| **Passes** | **Pass Duration** | | | | |
|---|---|---|---|---|---|
| **Per Week** | 30 min. | 1 hr. | 2 hrs. | 4 hrs. | 8 hrs. |
| 1 | (18.25, 11.58, 6.06) | (13.58, 6.05, 2.6) | (8.12, 1.67, 1.0) | (6.78, 0.55, 0.33) | (2.71, 0.36, 0.07) |
| 2 | (9.0, 6.97, 0.45) | (5.67, 2.5, 0.43) | (1.63, 1.01, 0.42) | (0.41, 0.33, 0.27) | (0.26, 0.21, 0.08) |
| 3 | (4.49, 2.65, 0.38) | (3.02, 1.87, 0.36) | (1.19, 0.81, 0.33) | (0.35, 0.26, 0.22) | (0.22, 0.18, 0.05) |
| 7 | (2.46, 1.65, 0.33) | (2.11, 1.07, 0.32) | (0.9, 0.58, 0.28) | (0.27, 0.21, 0.19) | (0.17, 0.12, 0.05) |

Table 17: Two-way Doppler plus monthly DDOR velocity reconstruction accuracy at data cut-off. Approximate values of the principal axes of the uncertainty ellipsoid, in mm/sec.

| **Passes** | **Pass Duration** | | | | |
|---|---|---|---|---|---|
| **Per Week** | 30 min. | 1 hr. | 2 hrs. | 4 hrs. | 8 hrs. |
| 1 | (44.26, 17.61, 0.99) | (23.52, 7.62, 0.5) | (6.97, 4.54, 0.2) | (5.3, 2.7, 0.05) | (4.57, 1.26, 0.01) |
| 2 | (21.05, 10.97, 0.68) | (14.26, 5.63, 0.29) | (3.93, 2.49, 0.11) | (1.21, 0.85, 0.03) | (0.58, 0.29, 0.01) |
| 3 | (7.61, 5.64, 0.41) | (6.23, 4.28, 0.21) | (2.87, 1.99, 0.09) | (0.95, 0.72, 0.05) | (0.52, 0.23, 0.03) |
| 7 | (3.73, 2.23, 0.23) | (3.13, 1.63, 0.13) | (1.45, 0.98, 0.06) | (0.5, 0.43, 0.03) | (0.27, 0.2, 0.02) |

Table 18: Two-way Doppler plus monthly DDOR position prediction accuracy at lunar close approach. Approximate values of the principal axes of the uncertainty ellipsoid, in km.

| **Passes** | **Pass Duration** | | | | |
|---|---|---|---|---|---|
| **Per Week** | 30 min. | 1 hr. | 2 hrs. | 4 hrs. | 8 hrs. |
| 1 | (89.3, 47.1, 23.2) | (75.0, 29.2, 15.9) | (49.4, 17.0, 14.6) | (43.4, 16.1, 14.4) | (37.1, 15.2, 14.3) |
| 2 | (45.4, 24.5, 17.9) | (39.0, 20.9, 15.0) | (35.7, 15.4, 14.0) | (35.4, 14.9, 13.7) | (35.4, 14.9, 13.7) |
| 3 | (36.3, 16.8, 15.3) | (35.9, 16.4, 14.6) | (35.5, 15.2, 13.9) | (35.4, 14.9, 13.7) | (35.4, 14.9, 13.7) |
| 7 | (21.6, 13.8, 11.0) | (21.4, 13.2, 10.9) | (20.5, 11.3, 10.7) | (17.1, 10.0, 9.3) | (15.2, 9.1, 8.6) |

Table 19: Two-way Doppler plus monthly DDOR velocity prediction accuracy at lunar close approach. Approximate values of the principal axes of the uncertainty ellipsoid, in mm/sec.

| **Passes** | **Pass Duration** | | | | |
|---|---|---|---|---|---|
| **Per Week** | 30 min. | 1 hr. | 2 hrs. | 4 hrs. | 8 hrs. |
| 1 | (463.9, 124.8, 65.3) | (394.6, 73.7, 38.2) | (258.3, 38.1, 32.6) | (226.6, 35.3, 31.7) | (197.2, 31.7, 30.6) |
| 2 | (236.6, 60.9, 47.3) | (208.4, 49.3, 34.2) | (190.7, 31.6, 30.3) | (189.2, 30.3, 28.8) | (189.1, 30.2, 28.7) |
| 3 | (194.3, 36.7, 35.0) | (192.2, 34.8, 32.5) | (189.8, 30.9, 29.7) | (189.2, 30.2, 28.8) | (189.1, 30.2, 28.7) |
| 7 | (113.3, 29.7, 22.3) | (112.5, 27.8, 21.8) | (109.2, 22.3, 20.5) | (95.0, 17.5, 16.3) | (85.8, 15.3, 12.9) |

Table 20: Two-way Doppler plus weekly DDOR position reconstruction accuracy at data cut-off. Approximate values of the principal axes of the uncertainty ellipsoid, in km.

| **Passes** | **Pass Duration** | | | | |
|---|---|---|---|---|---|
| **Per Week** | 30 min. | 1 hr. | 2 hrs. | 4 hrs. | 8 hrs. |
| 1 | (15.47, 6.87, 0.67) | (14.04, 2.55, 0.41) | (7.29, 1.0, 0.36) | (2.15, 0.48, 0.29) | (1.39, 0.29, 0.08) |
| 2 | (6.49, 0.65, 0.07) | (2.33, 0.37, 0.06) | (0.98, 0.33, 0.2) | (0.4, 0.28, 0.08) | (0.25, 0.21, 0.02) |
| 3 | (3.42, 0.67, 0.28) | (1.93, 0.39, 0.25) | (0.8, 0.27, 0.15) | (0.34, 0.22, 0.06) | (0.22, 0.18, 0.02) |
| 7 | (1.88, 0.71, 0.26) | (1.11, 0.44, 0.25) | (0.57, 0.26, 0.21) | (0.26, 0.19, 0.1) | (0.17, 0.12, 0.04) |

Table 21: Two-way Doppler plus weekly DDOR velocity reconstruction accuracy at data cut-off. Approximate values of the principal axes of the uncertainty ellipsoid, in mm/sec.

| **Passes** | **Pass Duration** | | | | |
|---|---|---|---|---|---|
| **Per Week** | 30 min. | 1 hr. | 2 hrs. | 4 hrs. | 8 hrs. |
| 1 | (17.54, 8.55, 0.48) | (7.66, 5.85, 0.31) | (5.57, 4.97, 0.15) | (5.14, 3.91, 0.05) | (4.49, 1.34, 0.02) |
| 2 | (10.72, 6.44, 0.14) | (5.95, 2.63, 0.11) | (2.97, 1.26, 0.05) | (1.2, 0.74, 0.03) | (0.7, 0.26, 0.02) |
| 3 | (7.35, 3.37, 0.12) | (5.01, 1.95, 0.08) | (2.4, 1.01, 0.06) | (0.97, 0.57, 0.05) | (0.58, 0.21, 0.03) |
| 7 | (2.83, 1.87, 0.08) | (1.88, 1.14, 0.07) | (1.11, 0.72, 0.05) | (0.5, 0.4, 0.03) | (0.28, 0.2, 0.02) |

Table 22: Two-way Doppler plus weekly DDOR position prediction accuracy at lunar close approach. Approximate values of the principal axes of the uncertainty ellipsoid, in km.

| **Passes** | **Pass Duration** | | | | |
|---|---|---|---|---|---|
| **Per Week** | 30 min. | 1 hr. | 2 hrs. | 4 hrs. | 8 hrs. |
| 1 | (69.3, 23.0, 18.7) | (66.6, 17.1, 15.7) | (46.5, 16.4, 14.6) | (37.3, 15.6, 14.4) | (36.4, 15.1, 14.1) |
| 2 | (35.8, 18.2, 16.4) | (35.6, 15.3, 14.9) | (35.5, 15.0, 14.0) | (35.4, 14.9, 13.7) | (35.4, 14.9, 13.7) |
| 3 | (35.6, 15.6, 15.5) | (35.5, 15.1, 14.6) | (35.4, 14.9, 13.9) | (35.4, 14.9, 13.7) | (35.4, 14.9, 13.7) |
| 7 | (21.1, 13.8, 10.9) | (21.0, 13.2, 10.8) | (20.5, 11.3, 10.6) | (16.8, 9.9, 9.3) | (15.2, 9.1, 8.6) |

Table 23: Two-way Doppler plus weekly DDOR velocity prediction accuracy at lunar close approach. Approximate values of the principal axes of the uncertainty ellipsoid, in mm/sec.

| **Passes** | **Pass Duration** | | | | |
|---|---|---|---|---|---|
| **Per Week** | 30 min. | 1 hr. | 2 hrs. | 4 hrs. | 8 hrs. |
| 1 | (356.9, 64.3, 42.6) | (344.4, 40.4, 35.2) | (245.0, 35.8, 31.8) | (199.8, 32.2, 30.6) | (195.2, 31.4, 29.1) |
| 2 | (190.9, 46.9, 34.6) | (189.9, 34.0, 30.8) | (189.5, 30.7, 29.5) | (189.2, 30.3, 28.8) | (189.1, 30.2, 28.7) |
| 3 | (190.1, 36.4, 31.7) | (189.6, 32.6, 30.3) | (189.3, 30.5, 29.2) | (189.1, 30.2, 28.7) | (189.1, 30.2, 28.7) |
| 7 | (111.3, 29.7, 21.5) | (111.0, 27.7, 20.9) | (109.2, 22.3, 20.5) | (93.8, 17.3, 16.1) | (85.7, 15.3, 12.8) |

Table 24: One-way Doppler-only position reconstruction accuracy at data cut-off. Approximate values of the principal axes of the uncertainty ellipsoid, in km.

| **Passes** | **Pass Duration** | | | | |
|---|---|---|---|---|---|
| **Per Week** | 30 min. | 1 hr. | 2 hrs. | 4 hrs. | 8 hrs. |
| 1 | (147.23, 61.13, 16.99) | (78.52, 26.44, 14.55) | (18.11, 15.12, 7.6) | (13.36, 3.19, 2.93) | (12.36, 1.22, 0.6) |
| 2 | (97.63, 44.33, 6.67) | (53.7, 18.3, 5.35) | (13.18, 8.15, 3.53) | (3.24, 2.72, 0.99) | (1.23, 0.61, 0.35) |
| 3 | (38.92, 13.29, 2.56) | (17.24, 8.73, 1.98) | (7.63, 4.85, 1.53) | (2.46, 2.06, 0.7) | (0.99, 0.49, 0.28) |
| 7 | (17.06, 6.44, 2.05) | (7.92, 4.81, 1.47) | (4.06, 3.35, 1.04) | (1.79, 1.47, 0.48) | (0.79, 0.36, 0.24) |

Table 25: One-way Doppler-only velocity reconstruction accuracy at data cut-off. Approximate values of the principal axes of the uncertainty ellipsoid, in mm/sec.

| **Passes** | **Pass Duration** | | | | |
|---|---|---|---|---|---|
| **Per Week** | 30 min. | 1 hr. | 2 hrs. | 4 hrs. | 8 hrs. |
| 1 | (138.09, 71.38, 4.89) | (80.66, 42.28, 3.39) | (33.07, 19.37, 1.15) | (10.51, 8.44, 0.35) | (7.41, 5.52, 0.2) |
| 2 | (74.07, 38.21, 3.5) | (36.6, 25.12, 2.41) | (17.62, 11.58, 1.0) | (6.54, 5.21, 0.26) | (3.06, 1.46, 0.09) |
| 3 | (32.73, 14.28, 2.22) | (17.52, 11.35, 0.97) | (9.2, 7.81, 0.48) | (5.41, 3.54, 0.19) | (2.49, 1.16, 0.09) |
| 7 | (10.88, 8.03, 1.65) | (7.85, 6.37, 0.71) | (5.52, 4.69, 0.35) | (3.05, 2.19, 0.16) | (1.37, 0.72, 0.1) |

Table 26: One-way Doppler-only position prediction accuracy at lunar close approach. Approximate values of the principal axes of the uncertainty ellipsoid, in km.

| **Passes** | **Pass Duration** | | | | |
|---|---|---|---|---|---|
| **Per Week** | 30 min. | 1 hr. | 2 hrs. | 4 hrs. | 8 hrs. |
| 1 | (393.8, 86.5, 45.3) | (217.5, 54.7, 41.6) | (83.2, 38.2, 24.6) | (69.7, 18.6, 16.2) | (66.0, 16.3, 14.8) |
| 2 | (223.0, 60.1, 24.9) | (125.2, 33.5, 24.2) | (46.6, 23.4, 18.5) | (36.1, 16.3, 15.2) | (35.4, 15.0, 14.0) |
| 3 | (46.3, 37.7, 21.0) | (39.4, 24.4, 19.4) | (37.2, 18.0, 16.5) | (35.7, 15.6, 14.7) | (35.4, 15.0, 13.9) |
| 7 | (24.6, 19.2, 12.0) | (23.3, 16.4, 11.6) | (22.3, 14.7, 11.3) | (20.9, 13.5, 10.8) | (18.5, 12.0, 10.3) |

Table 27: One-way Doppler-only velocity prediction accuracy at lunar close approach. Approximate values of the principal axes of the uncertainty ellipsoid, in mm/sec.

| **Passes** | **Pass Duration** | | | | |
|---|---|---|---|---|---|
| **Per Week** | 30 min. | 1 hr. | 2 hrs. | 4 hrs. | 8 hrs. |
| 1 | (1997.1, 279.8, 129.1) | (1108.3, 157.1, 123.4) | (435.6, 102.1, 70.0) | (364.7, 44.0, 38.3) | (345.4, 35.7, 32.7) |
| 2 | (1123.9, 197.8, 61.5) | (641.0, 100.3, 60.7) | (245.1, 56.9, 49.1) | (192.8, 35.2, 34.1) | (189.4, 31.0, 29.5) |
| 3 | (235.2, 125.6, 52.0) | (211.3, 69.3, 46.3) | (199.3, 41.4, 39.7) | (190.6, 33.2, 32.0) | (189.3, 30.7, 29.2) |
| 7 | (125.6, 54.1, 27.7) | (119.9, 40.2, 25.8) | (115.8, 33.2, 23.9) | (110.5, 28.7, 21.2) | (100.8, 24.3, 18.8) |

Table 28: One-way range-only position reconstruction accuracy at data cut-off. Approximate values of the principal axes of the uncertainty ellipsoid, in km.

| **Passes** | **Pass Duration** | | | | |
|---|---|---|---|---|---|
| **Per Week** | 30 min. | 1 hr. | 2 hrs. | 4 hrs. | 8 hrs. |
| 1 | (140.06, 10.95, 0.05) | (127.96, 9.71, 0.02) | (57.55, 9.4, 0.01) | (13.04, 7.14, 0.0) | (2.63, 1.63, 0.0) |
| 2 | (29.81, 5.08, 0.05) | (15.19, 1.79, 0.03) | (8.61, 0.75, 0.0) | (4.42, 0.32, 0.0) | (1.48, 0.21, 0.0) |
| 3 | (15.69, 2.99, 0.0) | (7.2, 1.18, 0.0) | (3.0, 0.55, 0.0) | (1.33, 0.24, 0.0) | (0.76, 0.13, 0.0) |
| 7 | (1.89, 0.31, 0.01) | (0.71, 0.24, 0.0) | (0.33, 0.19, 0.0) | (0.16, 0.13, 0.0) | (0.1, 0.07, 0.0) |

Table 29: One-way range-only velocity reconstruction accuracy at data cut-off. Approximate values of the principal axes of the uncertainty ellipsoid, in mm/sec.

| **Passes** | **Pass Duration** | | | | |
|---|---|---|---|---|---|
| **Per Week** | 30 min. | 1 hr. | 2 hrs. | 4 hrs. | 8 hrs. |
| 1 | (131.24, 39.34, 5.5) | (121.35, 38.31, 4.9) | (70.81, 37.24, 3.57) | (32.45, 27.12, 0.95) | (7.61, 6.89, 0.26) |
| 2 | (30.27, 10.59, 2.72) | (14.22, 4.37, 1.73) | (7.17, 2.15, 0.82) | (4.39, 1.11, 0.33) | (2.98, 0.67, 0.11) |
| 3 | (11.05, 6.34, 0.8) | (6.66, 4.44, 0.29) | (4.82, 1.81, 0.12) | (2.69, 0.85, 0.07) | (1.85, 0.52, 0.05) |
| 7 | (0.97, 0.65, 0.44) | (0.81, 0.49, 0.21) | (0.63, 0.41, 0.12) | (0.41, 0.32, 0.09) | (0.29, 0.22, 0.06) |

 

Table 30: One-way range-only position prediction accuracy at lunar close approach. Approximate values of the principal axes of the uncertainty ellipsoid, in km.

| **Passes** | **Pass Duration** | | | | |
|---|---|---|---|---|---|
| **Per Week** | 30 min. | 1 hr. | 2 hrs. | 4 hrs. | 8 hrs. |
| 1 | (155.8, 84.4, 23.3) | (145.4, 80.8, 22.9) | (94.3, 69.4, 22.1) | (71.7, 32.9, 20.8) | (37.5, 16.5, 15.6) |
| 2 | (41.6, 34.0, 18.6) | (36.5, 20.2, 15.4) | (35.6, 16.0, 14.8) | (35.4, 15.1, 14.4) | (35.4, 15.0, 14.0) |
| 3 | (38.4, 19.9, 15.1) | (35.9, 16.4, 14.9) | (35.5, 15.2, 14.4) | (35.4, 15.0, 13.9) | (35.4, 14.9, 13.8) |
| 7 | (20.9, 13.7, 10.8) | (20.9, 13.7, 10.7) | (20.8, 13.5, 10.7) | (20.8, 13.1, 10.7) | (20.5, 12.3, 10.7) |

Table 31: One-way range-only velocity prediction accuracy at lunar close approach. Approximate values of the principal axes of the uncertainty ellipsoid, in mm/sec.

| **Passes** | **Pass Duration** | | | | |
|---|---|---|---|---|---|
| **Per Week** | 30 min. | 1 hr. | 2 hrs. | 4 hrs. | 8 hrs. |
| 1 | (579.8, 411.6, 60.2) | (550.5, 385.4, 58.6) | (444.5, 249.6, 56.2) | (367.6, 97.3, 50.7) | (201.1, 37.4, 33.9) |
| 2 | (218.1, 109.4, 42.3) | (197.2, 53.8, 31.8) | (190.9, 38.6, 29.8) | (189.4, 33.6, 29.4) | (189.2, 31.2, 29.1) |
| 3 | (206.2, 51.9, 32.7) | (192.6, 38.5, 31.1) | (189.7, 33.2, 29.7) | (189.2, 30.9, 29.1) | (189.1, 30.5, 28.8) |
| 7 | (110.5, 29.1, 21.1) | (110.5, 28.9, 20.8) | (110.5, 28.4, 20.7) | (110.4, 27.2, 20.7) | (108.9, 25.3, 20.5) |

Table 32: One-way Doppler+range position reconstruction accuracy at data cut-off. Approximate values of the principal axes of the uncertainty ellipsoid, in km.

| **Passes** | **Pass Duration** | | | | |
|---|---|---|---|---|---|
| **Per Week** | 30 min. | 1 hr. | 2 hrs. | 4 hrs. | 8 hrs. |
| 1 | (53.2, 9.43, 0.0) | (21.52, 8.97, 0.0) | (8.28, 6.64, 0.0) | (3.05, 2.16, 0.0) | (1.17, 0.51, 0.0) |
| 2 | (7.03, 0.33, 0.01) | (5.57, 0.25, 0.01) | (3.25, 0.25, 0.0) | (1.62, 0.21, 0.0) | (0.9, 0.19, 0.0) |
| 3 | (1.74, 0.31, 0.0) | (1.33, 0.23, 0.0) | (1.05, 0.18, 0.0) | (0.82, 0.14, 0.0) | (0.59, 0.11, 0.0) |
| 7 | (0.27, 0.19, 0.0) | (0.21, 0.15, 0.0) | (0.16, 0.11, 0.0) | (0.13, 0.08, 0.0) | (0.09, 0.06, 0.0) |

Table 33: One-way Doppler+range velocity reconstruction accuracy at data cut-off. Approximate values of the principal axes of the uncertainty ellipsoid, in mm/sec.

| **Passes** | **Pass Duration** | | | | |
|---|---|---|---|---|---|
| **Per Week** | 30 min. | 1 hr. | 2 hrs. | 4 hrs. | 8 hrs. |
| 1 | (67.76, 37.28, 3.43) | (45.2, 34.32, 1.58) | (29.51, 19.0, 0.63) | (9.44, 8.29, 0.3) | (5.45, 2.38, 0.12) |
| 2 | (5.42, 1.55, 0.5) | (4.73, 1.25, 0.38) | (3.72, 0.9, 0.24) | (3.07, 0.69, 0.12) | (2.28, 0.59, 0.06) |
| 3 | (3.26, 1.06, 0.08) | (2.66, 0.84, 0.07) | (2.24, 0.68, 0.06) | (1.94, 0.54, 0.05) | (1.58, 0.43, 0.05) |
| 7 | (0.64, 0.42, 0.1) | (0.5, 0.35, 0.09) | (0.4, 0.29, 0.08) | (0.33, 0.24, 0.07) | (0.27, 0.2, 0.06) |

Table 34: One-way Doppler+range position prediction accuracy at lunar close approach. Approximate values of the principal axes of the uncertainty ellipsoid, in km.

| **Passes** | **Pass Duration** | | | | |
|---|---|---|---|---|---|
| **Per Week** | 30 min. | 1 hr. | 2 hrs. | 4 hrs. | 8 hrs. |
| 1 | (93.1, 67.2, 22.0) | (86.0, 44.9, 21.2) | (68.1, 24.5, 20.6) | (39.4, 17.2, 16.1) | (35.6, 15.1, 14.7) |
| 2 | (35.5, 15.3, 14.6) | (35.4, 15.1, 14.5) | (35.4, 15.0, 14.2) | (35.4, 15.0, 14.0) | (35.4, 14.9, 13.8) |
| 3 | (35.4, 15.0, 14.0) | (35.4, 15.0, 13.9) | (35.4, 15.0, 13.8) | (35.4, 14.9, 13.8) | (35.4, 14.9, 13.7) |
| 7 | (20.8, 13.3, 10.7) | (20.8, 13.1, 10.7) | (20.8, 12.9, 10.7) | (20.6, 12.4, 10.7) | (18.0, 11.3, 10.2) |

Table 35: One-way Doppler+range velocity prediction accuracy at lunar close approach. Approximate values of the principal axes of the uncertainty ellipsoid, in mm/sec.

| **Passes** | **Pass Duration** | | | | |
|---|---|---|---|---|---|
| **Per Week** | 30 min. | 1 hr. | 2 hrs. | 4 hrs. | 8 hrs. |
| 1 | (444.9, 236.7, 55.9) | (432.1, 139.3, 52.7) | (350.7, 69.2, 49.7) | (211.4, 38.9, 36.6) | (190.4, 33.0, 30.2) |
| 2 | (189.8, 36.4, 29.5) | (189.5, 34.7, 29.5) | (189.3, 32.3, 29.3) | (189.2, 31.3, 29.2) | (189.2, 30.6, 29.0) |
| 3 | (189.3, 31.4, 29.2) | (189.2, 30.9, 29.1) | (189.2, 30.7, 28.9) | (189.2, 30.5, 28.9) | (189.1, 30.4, 28.8) |
| 7 | (110.4, 27.7, 20.7) | (110.4, 27.3, 20.7) | (110.3, 26.6, 20.6) | (109.8, 25.4, 20.6) | (98.6, 22.3, 18.3) |

Table 36: One-way Doppler plus monthly DDOR position reconstruction accuracy at data cut-off. Approximate values of the principal axes of the uncertainty ellipsoid, in km.

| **Passes** | **Pass Duration** | | | | |
|---|---|---|---|---|---|
| **Per Week** | 30 min. | 1 hr. | 2 hrs. | 4 hrs. | 8 hrs. |
| 1 | (80.71, 20.2, 8.15) | (30.07, 18.51, 7.77) | (15.82, 10.07, 5.98) | (9.55, 2.94, 2.4) | (6.42, 1.12, 0.57) |
| 2 | (64.64, 11.62, 0.92) | (23.25, 9.42, 0.68) | (9.15, 8.03, 0.6) | (2.88, 2.62, 0.5) | (1.12, 0.58, 0.35) |
| 3 | (13.3, 6.13, 0.69) | (8.76, 4.55, 0.52) | (5.34, 3.46, 0.43) | (2.08, 1.87, 0.38) | (0.92, 0.46, 0.28) |
| 7 | (7.1, 6.14, 0.6) | (5.09, 4.6, 0.49) | (3.44, 3.3, 0.41) | (1.69, 1.43, 0.35) | (0.77, 0.35, 0.24) |

Table 37: One-way Doppler plus monthly DDOR velocity reconstruction accuracy at data cut-off. Approximate values of the principal axes of the uncertainty ellipsoid, in mm/sec.

| **Passes** | **Pass Duration** | | | | |
|---|---|---|---|---|---|
| **Per Week** | 30 min. | 1 hr. | 2 hrs. | 4 hrs. | 8 hrs. |
| 1 | (92.09, 45.49, 4.78) | (50.64, 39.99, 2.48) | (31.45, 19.31, 0.96) | (9.73, 8.44, 0.33) | (5.81, 3.82, 0.08) |
| 2 | (67.47, 24.56, 3.44) | (30.35, 21.1, 1.69) | (17.41, 11.58, 0.76) | (6.54, 5.19, 0.26) | (3.03, 1.46, 0.06) |
| 3 | (20.43, 13.69, 1.27) | (13.17, 9.66, 0.85) | (9.16, 6.63, 0.48) | (5.41, 3.5, 0.19) | (2.46, 1.15, 0.07) |
| 7 | (10.69, 8.0, 0.91) | (7.61, 6.37, 0.6) | (5.44, 4.69, 0.35) | (3.05, 2.18, 0.16) | (1.34, 0.7, 0.09) |

Table 38: One-way Doppler plus monthly DDOR position prediction accuracy at lunar close approach. Approximate values of the principal axes of the uncertainty ellipsoid, in km.

| **Passes** | **Pass Duration** | | | | |
|---|---|---|---|---|---|
| **Per Week** | 30 min. | 1 hr. | 2 hrs. | 4 hrs. | 8 hrs. |
| 1 | (193.1, 59.6, 44.4) | (106.2, 52.0, 40.7) | (80.8, 36.7, 24.6) | (56.5, 18.6, 16.2) | (42.9, 16.2, 14.8) |
| 2 | (132.9, 40.1, 24.0) | (61.4, 31.1, 22.9) | (42.4, 23.4, 18.4) | (36.0, 16.3, 15.1) | (35.4, 15.0, 14.0) |
| 3 | (41.0, 24.6, 20.9) | (38.5, 19.4, 18.2) | (36.7, 17.7, 15.9) | (35.6, 15.5, 14.7) | (35.4, 15.0, 13.9) |
| 7 | (24.6, 18.1, 12.0) | (23.2, 16.0, 11.6) | (22.2, 14.7, 11.2) | (20.9, 13.5, 10.8) | (18.5, 12.0, 10.3) |

Table 39: One-way Doppler plus monthly DDOR velocity prediction accuracy at lunar close approach. Approximate values of the principal axes of the uncertainty ellipsoid, in mm/sec.

| **Passes** | **Pass Duration** | | | | |
|---|---|---|---|---|---|
| **Per Week** | 30 min. | 1 hr. | 2 hrs. | 4 hrs. | 8 hrs. |
| 1 | (930.2, 188.8, 128.3) | (535.4, 145.1, 122.8) | (423.7, 95.1, 70.0) | (296.7, 43.3, 38.3) | (224.9, 35.7, 32.7) |
| 2 | (621.3, 132.5, 61.4) | (302.6, 93.7, 60.7) | (223.4, 56.8, 49.1) | (192.4, 35.1, 34.1) | (189.4, 31.0, 29.5) |
| 3 | (217.7, 63.0, 51.1) | (205.0, 47.9, 43.1) | (196.5, 39.9, 37.1) | (190.5, 33.1, 31.9) | (189.3, 30.7, 29.2) |
| 7 | (125.5, 44.8, 27.7) | (119.5, 37.8, 25.7) | (115.5, 33.0, 23.9) | (110.5, 28.7, 21.2) | (100.7, 24.3, 18.8) |

 

Table 40: One-way Doppler plus weekly DDOR position reconstruction accuracy at data cut-off. Approximate values of the principal axes of the uncertainty ellipsoid, in km.

| **Passes** | **Pass Duration** | | | | |
|---|---|---|---|---|---|
| **Per Week** | 30 min. | 1 hr. | 2 hrs. | 4 hrs. | 8 hrs. |
| 1 | (49.44, 12.31, 1.75) | (26.33, 11.78, 1.35) | (15.5, 7.56, 0.7) | (10.75, 2.96, 0.42) | (3.99, 1.18, 0.35) |
| 2 | (29.4, 2.01, 0.1) | (17.06, 1.45, 0.09) | (8.03, 1.05, 0.34) | (3.01, 0.51, 0.29) | (1.22, 0.33, 0.15) |
| 3 | (10.21, 2.06, 0.37) | (6.99, 1.45, 0.34) | (4.39, 0.77, 0.31) | (2.24, 0.4, 0.25) | (0.98, 0.26, 0.11) |
| 7 | (8.92, 2.26, 0.39) | (6.12, 1.71, 0.35) | (3.66, 1.09, 0.31) | (1.75, 0.54, 0.27) | (0.78, 0.23, 0.18) |

Table 41: One-way Doppler plus weekly DDOR velocity reconstruction accuracy at data cut-off. Approximate values of the principal axes of the uncertainty ellipsoid, in mm/sec.

| **Passes** | **Pass Duration** | | | | |
|---|---|---|---|---|---|
| **Per Week** | 30 min. | 1 hr. | 2 hrs. | 4 hrs. | 8 hrs. |
| 1 | (69.54, 28.85, 0.6) | (42.31, 18.87, 0.57) | (19.18, 8.98, 0.5) | (8.31, 5.93, 0.31) | (5.46, 5.16, 0.15) |
| 2 | (50.64, 16.36, 0.24) | (27.29, 13.09, 0.2) | (11.44, 6.78, 0.16) | (6.19, 2.7, 0.12) | (2.98, 1.1, 0.08) |
| 3 | (21.56, 8.15, 0.23) | (14.09, 6.24, 0.19) | (8.26, 4.18, 0.14) | (5.28, 2.07, 0.1) | (2.43, 0.88, 0.08) |
| 7 | (10.7, 6.39, 0.22) | (7.81, 4.73, 0.18) | (5.29, 2.87, 0.15) | (3.03, 1.34, 0.12) | (1.33, 0.61, 0.09) |

Table 42: One-way Doppler plus weekly DDOR position prediction accuracy at lunar close approach. Approximate values of the principal axes of the uncertainty ellipsoid, in km.

| **Passes** | **Pass Duration** | | | | |
|---|---|---|---|---|---|
| **Per Week** | 30 min. | 1 hr. | 2 hrs. | 4 hrs. | 8 hrs. |
| 1 | (91.3, 62.5, 36.2) | (73.2, 45.6, 27.6) | (68.9, 24.5, 18.8) | (56.6, 17.1, 15.8) | (40.2, 15.8, 14.7) |
| 2 | (62.7, 34.6, 23.5) | (39.9, 31.0, 20.8) | (35.9, 19.0, 16.6) | (35.6, 15.3, 15.0) | (35.4, 15.0, 14.0) |
| 3 | (38.2, 24.9, 18.2) | (36.3, 19.8, 16.9) | (35.7, 16.2, 15.8) | (35.5, 15.1, 14.7) | (35.4, 14.9, 13.9) |
| 7 | (22.4, 18.5, 12.0) | (21.7, 16.3, 11.5) | (21.2, 14.7, 11.0) | (20.8, 13.5, 10.8) | (18.3, 12.0, 10.3) |

Table 43: One-way Doppler plus weekly DDOR velocity prediction accuracy at lunar close approach. Approximate values of the principal axes of the uncertainty ellipsoid, in mm/sec.

| **Passes** | **Pass Duration** | | | | |
|---|---|---|---|---|---|
| **Per Week** | 30 min. | 1 hr. | 2 hrs. | 4 hrs. | 8 hrs. |
| 1 | (376.5, 251.5, 86.6) | (365.2, 146.7, 65.9) | (354.6, 69.7, 43.0) | (294.8, 41.4, 34.6) | (214.3, 33.8, 31.5) |
| 2 | (221.8, 159.9, 54.1) | (196.7, 99.9, 46.6) | (191.1, 50.0, 35.1) | (189.8, 34.9, 30.7) | (189.3, 31.0, 29.3) |
| 3 | (197.2, 70.8, 40.1) | (192.7, 51.7, 36.2) | (190.4, 38.8, 32.4) | (189.6, 33.2, 30.3) | (189.2, 30.7, 29.1) |
| 7 | (114.6, 47.9, 26.6) | (113.0, 39.3, 24.4) | (111.7, 33.1, 22.3) | (110.3, 28.7, 20.9) | (99.9, 24.2, 18.6) |